REPORT DOCUMENTATION PAGE

Form Approved
OMB No. 074-0188

1. AGENCY USE ONLY (Leave blank)	2. REPORT DATE	3. REPORT TYPE AND DATES COVERED
	June 1996	

4. TITLE AND SUBTITLE
Progress in Developing an Open Burn/Open Detonation Dispersion Model

5. FUNDING NUMBERS
N/A

6. AUTHOR(S)
J.C. Weil, Brian D. Templeman, W. Mitchell

7. PERFORMING ORGANIZATION NAME(S) AND ADDRESS(ES)
University of Colorado
Boulder, CO

US Environmental Protection Agency
Research Triangle Park, NC

8. PERFORMING ORGANIZATION REPORT NUMBER
N/A

9. SPONSORING / MONITORING AGENCY NAME(S) AND ADDRESS(ES)
SERDP
901 North Stuart St. Suite 303
Arlington, VA 22203

Air & Waste Management Association

10. SPONSORING / MONITORING AGENCY REPORT NUMBER
96-TA35.01

11. SUPPLEMENTARY NOTES
For Presentation at the 89th Annual Meeting & Exhibition, Nashville, Tennessee, June 23-28, 1996.

12a. DISTRIBUTION / AVAILABILITY STATEMENT
Approved for public release: distribution is unlimited.

12b. DISTRIBUTION CODE
A

13. ABSTRACT ***(Maximum 200 Words)***

14. SUBJECT TERMS
open burning
open detonation
dispersion model
SERDP
SERDP Collection

15. NUMBER OF PAGES
15

16. PRICE CODE N/A

17. SECURITY CLASSIFICATION OF REPORT	18. SECURITY CLASSIFICATION OF THIS PAGE	19. SECURITY CLASSIFICATION OF ABSTRACT	20. LIMITATION OF ABSTRACT
unclass.	unclass.	unclass.	UL

96-TA35.01

Progress in Developing an Open Burn/ Open Detonation Dispersion Model

J.C. Weil
University of Colorado
Boulder, Colorado

B. Templeman
NOAA
Boulder, Colorado

W. Mitchell
U.S. Environmental Protection Agency
Research Triangle Park, North Carolina

AIR & WASTE MANAGEMENT
ASSOCIATION

SINCE 1907

For Presentation at the
89th Annual Meeting & Exhibition
Nashville, Tennessee
June 23-28, 1996

INTRODUCTION

Obsolete or unwanted munitions, rocket propellants, and manufacturing wastes require treatment at Department of Defense (DOD) and Department of Energy (DOE) facilities. One of the most widely-used treatment methods is open burning (OB) and open detonation (OD) of the material. Currently, the material destroyed in a single detonation generally ranges from 100 to 5000 lbs, while the quantity removed by a burn can be larger and last from minutes to an hour. OB/OD operations are confined to daytime with atmospheric stability conditions ranging from convective or highly unstable to near neutral.

OB/OD activities produce air pollutants and require predictions of pollutant concentrations to obtain an operating permit. The pollutants include SO_2, NO_x, particulates, volatile organic compounds and toxic materials such as metals, semivolatile organics, etc.[1] Large detonations also generate large quantities of dust/soil that are entrained by the rising contaminant cloud. OB/OD sources differ from most traditional air pollution sources in that they have: 1) instantaneous or short-duration releases of buoyant material rather than continuous releases, and 2) ambient exposure times for the clouds that can be much less than the typical averaging times ($\gtrsim 1$ hr) of air quality standards.

Atmospheric dispersion models are used to estimate pollutant concentrations given information on the source and meteorological conditions. However, there is currently no recommended EPA dispersion model to address the unique features of OB/OD sources. The most commonly-used approach is INPUFF,[2] a Gaussian puff model, but this has several limitations as briefly discussed below and elsewhere.[3] As a result, a model development program was initiated under the DOD/DOE Strategic Environmental Research and Development Program.

This paper briefly summarizes the model development effort which is divided into "operational" and "research" components. In the following, we give a brief discussion of the background and overall model design and then describe the operational model components for instantaneous (OD) and short-duration (OB) sources; the OD model is a Gaussian puff approach whereas the OB framework consists of integrated-puff and plume models. The combined OB/OD model includes: 1) a continuous treatment of dispersion as the release condition varies from instantaneous to continuous, 2) cloud and plume rise obtained from appropriate entrainment models, 3) cloud and plume penetration of elevated inversions, 4) relative (puff) and total dispersion based on modern scaling concepts for the planetary boundary layer (PBL), and 5) a capability for the use of onsite profiles of wind, temperature, and turbulence from a mobile meteorological platform. The current OB/OD model focuses on the unstable PBL.

BACKGROUND AND MODEL DESIGN

Background

The development of an OB/OD dispersion model has considered: 1) the limitations of existing models, 2) current knowledge of turbulence and dispersion in the PBL, and 3) a mobile meteorological platform under development.

Limitations of existing models. INPUFF has been used to model OB/OD sources and can handle dispersion from individual puffs or clouds or from a sequence of puffs in a short-duration release. Although the Gaussian puff approach is suitable for OB/OD sources, INPUFF has the following limitations: 1) It adopts dispersion parameters (σ_y, σ_z) from the Pasquill-Gifford (PG) curves. 2) It includes Briggs' (Ref. 4) plume rise expressions which apply to continuous releases rather than to instantaneous sources (puffs, clouds) and does not address thermal penetration of elevated inversions capping the PBL. 3) It assumes Gaussian velocity statistics for the turbulence, whereas the vertical velocity statistics in the unstable PBL are positively skewed.[5] The skewness should be included for vertical dispersion.

For OB/OD sources, the PG curves are deficient in that they: 1) are based on dispersion from a ground-level source and short downwind distances (< 1 km), and 2) are selected using surface meteorology, which does not account for the PBL's vertical structure. For large detonations, source buoyancy can carry emissions to several 100 m or the PBL top; one must then deal with dispersion over the entire PBL.

PBL turbulence. Dispersion in the PBL depends on the turbulence length and velocity scales which differ for the unstable or convective boundary layer (CBL) and the stable boundary layer (SBL). For the CBL, the length and velocity scales are the CBL depth h and the convective velocity scale w_*; $w_* = (g\overline{w\theta_o}h/\Theta_a$, where g is the gravitational acceleration, $\overline{w\theta_o}$ is the turbulent heat flux at the surface, and Θ_a is the ambient potential temperature. Typical values of w_* and h at midday over land are 1 - 2 m/s and 1 - 2 km. Within the "mixed layer" $(0.1h \leq z < h)$, the mean wind speed and turbulence components—longitudinal σ_u, lateral σ_v, and vertical σ_w—vary little with height z; in strong convection, $\sigma_u, \sigma_v, \sigma_w \simeq 0.6w_*$.

For the SBL, the turbulence is much weaker with eddy sizes proportional to z near the surface and typically $\sim$ 10s of meters or less in the upper part of the SBL. Models and observations show that the velocity scale is the friction velocity u_* (Ref. 5), which is typically $\sim$ 0.1 m/s in strong stable stratification.

Knowledge of the PBL turbulence structure has been included in a number of models for air quality applications.[6] One example is AERMOD[7] for industrial source complexes.

Mobile meteorological platform. A mobile meteorological platform is being developed at NOAA's Environmental Technology Laboratory to obtain the PBL variables necessary for modeling since many DOD facilities are in remote locations. The platform design includes: 1) a radar wind profiler for obtaining the three wind

components up to $\sim$ 3 km, 2) a radio acoustic sounding system (RASS) for temperature measurements, 3) a mini-SODAR for measuring winds and σ_w to a height of $\sim$ 200 m, 4) a mini-lidar system for obtaining the PBL depth h, and 5) a portable meteorological station for measuring near-surface winds, temperature, turbulence, and heat flux. The dispersion model is being designed for efficient use of these measurements.

Overall Model Design

The overall model design includes: 1) a simple computational or operational framework for routine problems, and 2) a more detailed or research model for nonroutine problems. In the operational approach, a Gaussian puff model is adopted for instantaneous sources and puff, integrated-puff, and plume models for short-duration releases. For the research framework, a Lagrangian particle and/or puff approach is planned. Both frameworks will be considered for "onsite" use in a real-time operational mode using data from the mobile meteorological platform, i.e., for day-to-day decisions on OB/OD operations. The operational puff and plume models would be used for climatological analyses needed in risk assessments.

In modeling, the important aspects to address are: 1) all source-related features including the instantaneous or short-duration nature of the release, buoyancy-induced rise and dispersion, and cloud or plume penetration of elevated inversions, 2) relative and absolute dispersion expressions that explicitly include PBL turbulence variables, 3) meteorological variables including their vertical profiles from the mobile platform, and 4) a treatment for puff and plume dispersion about complex terrain.

The models discussed in the following sections address points 1 and 2 above and must be expanded to include points 3 and 4. Further development also will address: 1) a more complete description of initial source effects (detonation cloud size and height) and inversion penetration, 2) a more complete PBL turbulence parameterization, 3) averaging time effects on concentration, 4) the entrained dust source term, and 5) deposition of gases and particles.

INSTANTANEOUS SOURCES

Dispersion Model

In many OB/OD applications, estimates of peak ground-level concentrations (GLCs) are required for averaging times ranging from seconds or minutes to an hour or longer. In making such estimates, we must account for the stochastic or random nature of turbulence and dispersion in the PBL. That is, we must recognize that the observed concentration at a receptor is a random variable and should be predicted statistically through a probability distribution.[8,9] The distribution can be parameterized by a functional form such as a gamma or clipped-normal distribution[9] and requires a minimum of two variables to characterize it—the mean concentration C and the root-mean-square (rms) concentration fluctuation σ_c, which is a measure of the width of the distribution. The peak concentration then can be defined by a specified percentile value of the cumulative probability distribution, e.g., the 99.9th percentile level. In the

following, we discuss approaches for predicting C, σ_c, cloud rise, and the dispersion parameters; the functional form of the distribution remains to be selected.

Mean concentration. For instantaneous sources or detonations, a Gaussian puff model is adopted for predicting the short-term mean concentration (C) field relative to the puff centroid. The C is the expected or average concentration that would be observed if the same experiment—same source and meteorological conditions—were repeated a large number of times.[9] The C is given by:

$$C = \frac{Q}{(2\pi)^{3/2}\sigma_{rx}\sigma_{ry}\sigma_{rz}} \exp\left[-\frac{(x-Ut)^2}{2\sigma_{rx}^2} - \frac{y^2}{2\sigma_{ry}^2} - \frac{(z-h_e)^2}{2\sigma_{rz}^2}\right], \qquad (1)$$

where Q is the pollutant mass released, U is the mean wind speed, t is the travel time, h_e is the effective puff height, and σ_{rx}, σ_{ry}, and σ_{rz} are the puff standard deviations or relative dispersion parameters in the x, y, and z directions, respectively. Here, $h_e = h_s + \Delta h(x)$ where h_s is the source height which is generally zero for OB/OD sources, and Δh is the cloud rise due to buoyancy; x and y are the distances in the mean wind and crosswind directions.

The maximum mean concentration C_c at the puff centroid is given by $C_c = Q/[(2\pi)^{3/2}\sigma_{rx}\sigma_{ry}\sigma_{rz}]$, where the relative dispersion parameters are generally different in the three directions. In the following, we assume $\sigma_{rx} = \sigma_{ry} = \sigma_{rz} = \sigma_r$.

The C field including puff meandering is given by Eq. (1), but with $\sigma_{rx}, \sigma_{ry}, \sigma_{rz}$ replaced by the absolute dispersion parameters—$\sigma_x, \sigma_y, \sigma_z$. A Gaussian distribution for C is applicable in the SBL where the probability density function (p.d.f.), p_w, of the vertical velocity w is Gaussian. However, for the CBL, a skewed w p.d.f. is more consistent with laboratory and field data. A skewed p.d.f. is adopted here and is parameterized by the superposition of two Gaussian distributions.[10]

The C field due to an ensemble of meandering puffs is derived from p_w following the same approach as applied to continuous plumes.[10] The resulting expression for C is

$$C = \frac{Q}{(2\pi)^{3/2}\sigma_x\sigma_y} \exp\left(-\frac{(x-Ut)^2}{2\sigma_x^2} - \frac{y^2}{2\sigma_y^2}\right) \times \sum_{j=1}^{2} \frac{\lambda_j}{\sigma_{zj}} \exp\left(-\frac{(z-h_e-\overline{z_j})^2}{2\sigma_{zj}^2}\right), \qquad (2)$$

where $\sigma_{zj} = \sigma_{wj}x/U$ and $\overline{z_j} = \overline{w_j}x/U$ with $j = 1, 2$. The λ_j, $\overline{w_j}$, and σ_{wj} $(j = 1, 2)$ are the weight, mean velocity, and standard deviation of each Gaussian p.d.f. comprising p_w. Equation (2) applies for short distances such that the plume interaction with the ground or elevated inversion is weak. The complete expression for C includes multiple cloud reflections at the ground and PBL top.

The time-averaged concentration can be found from the dose where the partial dose is defined by $\psi(x, y, z, t) = \int_0^t C(x, y, z, t')dt'$ and the total dose by $\psi_\infty = \psi(x, y, z, \infty)$. For clouds with short passage times over a receptor, the average concentration $\overline{C}$ can be obtained from $\overline{C} = (\psi(t_2) - \psi(t_1))/T_a$, where the averaging time $T_a = t_2 - t_1$. If the puff passage time $4\sigma_{rx}/U$ is less than T_a, then $\overline{C} = \psi_\infty/T_a$.

Rms concentration fluctuation. For elevated sources such as a buoyant cloud, the rms concentration fluctuation at the ground is largest close to the source and decreases with increasing distance.[9,11] As a first step in predicting σ_c, we adopt Gifford's[12] meandering plume or cloud model which applies to the near-source region; specifically, it applies when the large-scale eddies in the PBL cause the wandering or meandering of a small growing plume or cloud. The cloud only occasionally reaches the ground, but it does so in high concentration due to the small local spread σ_r; thus, it creates large "spikes" in the GLC distribution and a large concentration variance.[11] In the following, we model the mean square concentration $\langle c^2 \rangle$, where the angle brackets denote an ensemble average, and then find σ_c from $\sigma_c = (\langle c^2 \rangle - C^2)^{1/2}$ (see Ref. 9).

In Gifford's model, the instantaneous concentration distribution in a cloud is assumed to be a nonrandom, axisymmetric Gaussian distribution about the instantaneous cloud centroid $\boldsymbol{x}_c = (x_c, y_c, z_c)$:

$$c(\boldsymbol{x}, \boldsymbol{x}_c) = \frac{Q}{(2\pi)^{3/2}\sigma_r^3} \exp\left[-\frac{(x-x_c)^2}{2\sigma_r^2} - \frac{(y-y_c)^2}{2\sigma_r^2} - \frac{(z-z_c)^2}{2\sigma_r^2} \right] . \tag{3}$$

Concentration fluctuations arise due to the randomness in x_c, y_c and z_c, which is caused by the meandering of the cloud.

The $\langle c^2 \rangle$ is obtained by averaging the quantity c^2 from Eq. (3) over the joint displacement p.d.f., $p(\boldsymbol{x}_c, t)$, which is a function of time. In the well-mixed CBL, the turbulent velocity fluctuations in the x, y, z directions are uncorrelated throughout the bulk of the layer; likewise, the centroid displacements in the three directions should be uncorrelated random variables. Thus, assuming independence of the displacements in the three directions, we have $p(\boldsymbol{x}_c, t) = p_x(x_c, t) \cdot p_y(y_c, t) \cdot p_z(z_c, t)$. Using Gifford's approach, the $\langle c^2 \rangle$ is found from

$$\langle c^2 \rangle = \int_{x_c} \int_{y_c} \int_{z_c} c^2(\boldsymbol{x}; \boldsymbol{x}_c) p_x(x_c, t) \cdot p_y(y_c, t) \cdot p_z(z_c, t) dx_c dy_c dz_c . \tag{4}$$

The displacement p.d.f.s in (4) are found from the velocity p.d.f.s—$p_u(u)$, $p_v(v)$, and $p_w(w)$, where u, v, w are the random velocity components in the x, y, z directions. Close to the source, we assume that $x_c = ut$, $y_c = vt$, and $z_c = h_e + wt$. The p_x, p_y and p_z can then be derived as in Weil.[10] Taking p_u and p_v as Gaussian, one finds

$$p_x(x_c) = \frac{1}{\sqrt{2\pi}\sigma_x} \exp\left[-\frac{(x_c - \langle x_c \rangle)^2}{2\sigma_x^2} \right] , \quad p_y(y_c) = \frac{1}{\sqrt{2\pi}\sigma_y} \exp\left[-\frac{y_c^2}{2\sigma_y^2} \right] , \tag{5}$$

where $\sigma_x = \sigma_u t$, $\langle x_c \rangle = Ut$, and $\sigma_y = \sigma_v t$. For p_w, a bi-Gaussian p.d.f. or superposition of two Gaussian distributions is adopted, which results in a similar distribution for p_z as noted earlier (Eq. 2).

By substituting the derived p_x, p_y, and p_z into Eq. (4) and carrying out the integration, we obtain

$$\langle c^2 \rangle = \frac{Q^2}{(2\pi)^3 \sigma_r^3 \sigma_{xe} \sigma_{ye}} \exp\left(-\frac{(x-Ut)^2}{\sigma_{xe}^2} - \frac{y^2}{\sigma_{ye}^2} \right) \times \sum_{j=1}^{2} \frac{\lambda_j}{\sigma_{zej}} \exp\left(-\frac{(z - h_e - \overline{z_j})^2}{\sigma_{zej}^2} \right) , \tag{6}$$

where $\sigma_{xe} = (\sigma_r^2 + 2\sigma_x^2)^{1/2}$, $\sigma_{ye} = (\sigma_r^2 + 2\sigma_y^2)^{1/2}$, and $\sigma_{zej} = (\sigma_r^2 + 2\sigma_{zj}^2)^{1/2}$ with $j = 1$ or 2. The λ_j, $\overline{z_j}$, and σ_{zj} are the same variables as in Eq. (2). The above $\langle c^2 \rangle$ expression applies to short distances such that the cloud interaction with the ground and elevated inversion is weak; similar to Eq. (2), we include reflections at $z = 0, h$ to obtain the complete expression for $\langle c^2 \rangle$.

Note that Eq. (6) is of the same form as Eq. (2) except for the omission of the 2 in the denominator of the exponential terms. This is consistent with the $\langle c^2 \rangle$ expression for passive releases in Gaussian turbulence (see Refs. 11 and 12).

Cloud rise and inversion penetration. Scorer[13] combined theory and laboratory experiments to obtain the following expression for cloud rise in a neutral environment

$$\Delta h = 2.35(M_T t + F_T t^2)^{1/4} \ . \tag{7}$$

M_T and F_T are the initial momentum and buoyancy of the cloud and are given by

$$M_T = \frac{4\pi}{3} r_o^3 w_o \qquad \text{and} \qquad F_T = \frac{g Q_T}{c_p \rho_a \Theta_a} \ , \tag{8}$$

where w_o, r_o, and Q_T are the initial velocity, radius, and heat content of the thermal, c_p is the specific heat of air, and ρ_a and Θ_a are the ambient air density and potential temperature. The Q_T can be determined from the mass of the detonation and its heat content, $H = 1100$ kcal/kg TNT equivalent.

Scorer also found the puff radius to be $r = \alpha \Delta h_t$, where Δh_t is the cloud top height and α is an empirical entrainment coefficient. α ranged from 0.14 to 0.5 with a mean of 0.25. The relative dispersion $\sigma_r = r/\sqrt{2}$.

Using field observations, Weil[14] confirmed that Eq. (7) was a good fit to data over a wide range of times. Thus, Eq. (7) is suitable for the rise of a cloud before it is limited by stable stratification, e.g., an elevated inversion.

For cloud penetration of an elevated density jump, results have been found from laboratory experiments in a nonturbulent environment. Richards[15] obtained an empirical expression for the fraction P of the cloud penetrating the jump: $P \simeq 1 - 0.5\Delta\rho_i/\Delta\rho_{Ti}$, where $\Delta\rho_i$ is the density jump and $\Delta\rho_{Ti}$ is the average density excess of the cloud when it reaches the jump. This can be applied to atmospheric detonations and elevated temperature inversions by relating $\Delta\rho$ to the cloud temperature excess $\Delta\Theta$, expressing $\Delta\Theta$ in terms of F_T and r, and evaluating the resulting expression at $z = h$. From $\Delta\rho/\rho_a = \Delta\Theta/\Theta_a$ and the above approach, one finds $\Delta\Theta = (3/4\pi)Q_T/(\rho_a c_p r^3)$. Richards' expression can then be rewritten as $P = 1 - (2\pi/3)(\Delta\Theta_i \rho_a c_p \alpha^3 h^3/Q_T)$, where $\Delta\Theta_i$ is the temperature jump. The h_s is assumed to be zero so that the cloud radius at $z = h$ is αh. The above relationship shows the strong sensitivity of P to αh.

A more realistic temperature distribution above the CBL is a constant $\partial\Theta_a/\partial z$. Experiments simulating this distribution as well as a jump above a well-mixed layer are

currently underway in a salt-stratified tank at the EPA Fluid Modeling Facility in North Carolina.

Dispersion parameters. For clouds, σ_r is dominated by entrainment for short times with $\sigma_r = \sigma_{rb} = 0.18\Delta h$, where subscript b denotes buoyancy-induced spread. At intermediate times ($t < T_L$), the σ_r may be dominated by ambient turbulence in the inertial subrange with $\sigma_r \sim \sigma_{ra} = a_1\epsilon^{1/2}t^{3/2}$, where T_L is the Lagrangian time scale, ϵ is the turbulent kinetic energy dissipation rate, a_1 is a constant (see Thomson[16]), and subscript a denotes dispersion due to ambient turbulence. At long times ($t \gg T_L$), $\sigma_{ra} = (2\sigma_w^2 T_L t)^{1/2}$ for homogeneous isotropic turbulence. For σ_{ra}, we use an interpolation expression of the form $\sigma_{ra} = a_1\epsilon^{1/2}t^{3/2}/(1 + a_2 t/T_L)$ to satisfy the intermediate- and long-time results. In addition, ϵ can be written as $\epsilon = b\sigma_w^2/T_L$ in homogeneous isotropic turbulence.

In a strong CBL, the following approximations can be made for $z \geq 0.1h$: $\epsilon \simeq 0.4w_*^3/h$, $\sigma_w \simeq 0.6w_*$, and $T_L \sim 0.7h/w_*$ (Ref. 10). These approximations coupled with $\epsilon = b\sigma_w^2/T_L$ lead to $b = 0.78$. To satisfy the long-time σ_{ra} limit, we must have $a_2 = 0.62a_1$; a_1 is estimated to be 0.57 from Thomson's two-particle model results. The resulting parameterization for σ_{ra} in the CBL is

$$\frac{\sigma_{ra}}{h} = \frac{0.36X^{3/2}}{1+0.51X} \quad \text{with} \quad X = \frac{w_* x}{Uh}\,, \tag{9}$$

where we have assumed $t = x/U$ and X is a dimensionless distance or travel time.

To connect the short-, intermediate-, and long-time relative dispersion regimes in a continuous manner, we adopt the following parameterization: $\sigma_r^3 = \sigma_{rb}^3 + \sigma_{ra}^3$. For clouds dominated by buoyancy, $\sigma_{rb} = 0.42F_T^{1/4}t^{1/2}$.

The total or absolute dispersion is necessary to estimate the C for a meandering puff or plume. The σ_x and σ_y in Eq. (2) can be obtained from a parameterization of Taylor's theory: $\sigma_x = \sigma_u t/(1 + t/2T_{Lx})^{1/2}$ and similarly for σ_y. The T_{Lx} is the Lagrangian time scale for the u component and can be parameterized by $T_{Lx} \propto \sigma_u/h$, etc. (e.g., see Ref. 6). For the CBL and the results below, we use $T_{Lx} = T_{Ly} = 0.7h/w_*$ and $\sigma_u = \sigma_v = 0.6w_*$.

Example Results

We have computed the C_c in the buoyant puff and the mean GLC along $y = 0$ due to a meandering puff for $0.1 \leq W \leq 50$ tons. The σ_r, σ_x, and σ_y were calculated as described in the previous section. In the following, the cloud buoyancy is characterized by its dimensionless value

$$F_{T*} = \frac{F_T}{w_*^2 h^2}\,; \tag{10}$$

in the examples below, we use $w_* = 2$ m/s, $h = 1000$ m, and $U = 5$ m/s.

Figure 1 shows calculated values of the peak (C_c) SO_2 concentrations in a detonation cloud. The cloud SO_2 mass is estimated from $Q = W \cdot E_f$, where E_f ($= 2.23 \times 10^{-4}$;

Andrulis[1]) is the SO_2 emission factor. At small x, all of the curves have the same slope: $C_c \propto x^{-3/2}$ because $\sigma_{rb} \propto x^{1/2}$ and the σ_r is dominated by σ_{rb} near the source. For 200 m $< x \lesssim$ 2000 m, some curves exhibit a short region of a nearly constant C_c with x: this is due to puff trapping in the CBL and a temporary limitation on vertical dispersion due to the elevated inversion. At large distances ($x >$ 10 km), clouds for all cases become uniformly mixed in the vertical but continue to spread laterally. Thus, the C_c tends towards $Q/\sigma_{ra}^2 \propto Q/x$; the curves for W = 10 - 50 tons show that C_c varies inversely with x for large distances.

Figure 2 shows the mean GLC C along the puff centerline ($y = 0$) for the same range of W and F_T values as in Fig. 1. This mean is for an ensemble of meandering puffs and is obtained from Eq. (2) with reflection terms included. Several interesting features are found: 1) A non-monotonic variation occurs in the maximum GLC C_m with W and F_T. 2) The variation in C_m for $0.1 \leq W \leq 50$ tons is only about a factor of 4 even though the range in Q is a factor of 500; the weak dependence on Q is attributed to the increase in Δh with F_T. 3) The C_m is of the order of 0.1 μg/m^3, which is the lower bound for C_c in Fig. 1. 4) The increase in the distance to the maximum concentration with W is due to the increase in Δh with F_T or W.

For $\sigma_c \gtrsim C$, the mean GLC along $y = 0$ due to an ensemble of meandering puffs probably has little to do with the observed centerline GLC in an individual puff. This is attributed to the large variability in individual concentration observations when $\sigma_c \gtrsim C$. As noted earlier, the computed C in Fig. 2 would be used together with a modeled σ_c in a concentration probability distribution to estimate the peak short-term GLC that could occur downstream of the detonation.

Some preliminary calculations of σ_c/C at the distance of the maximum GLC were made for the examples in Fig. 2. For $W = 0.1, 1$, and 5 tons, the corresponding σ_c/C was 6, 2, and 1.8; for W = 10 to 50 tons, the $\sigma_c/C \lesssim 1$ and was decreasing rapidly with increasing distance. The rapid decrease was attributed to the large cloud size (σ_r) relative to h and the approach of the concentration distribution to a vertically well-mixed value. The σ_c model requires generalization to address the σ_c at large distances: $x \gtrsim (2 - 3)Uh/w_*$, or about 5 - 7.5 km in the current example. This will be pursued in the future.

SHORT-DURATION RELEASES

Dispersion Model

For short-duration releases or burns, our general approach is an integrated puff model in which the short-term mean concentration relative to the puff centerline is

$$C = \int_0^{t_r} \frac{Q_r \, f(\boldsymbol{x}, t, t') \, dt'}{(2\pi)^{3/2} \sigma_{rx} \sigma_{ry} \sigma_{rz}} \tag{11a}$$

$$f = \exp\left[-\frac{(x - U(t - t'))^2}{2\sigma_{rx}^2} - \frac{y^2}{2\sigma_{ry}^2} - \frac{(z - h_e)^2}{2\sigma_{rz}^2} \right] , \tag{11b}$$

where $\boldsymbol{x} = (x, y, z)$, t' is the puff emission time, t_r is the total release duration, Q_r is the continuous source emission rate, $\sigma_{rx} = \sigma_{rx}(t - t')$, and similarly for σ_{ry}, σ_{rz}. The integration in (11a) can be carried out analytically for limiting forms of $\sigma_{rx}(t - t')$, etc., but must be done numerically in general.

The integrated puff model also is used for estimating the mean concentration due to a sequence of meandering puffs by replacing the relative dispersion (σ_{rx}, etc in Eq. 11) by the absolute dispersion—σ_x, σ_y, σ_z.

In the following, we calculate the C_c for a short-duration release by numerically integrating Eq. (11) with $\sigma_{rx} = \sigma_{ry} = \sigma_{rz} = \sigma_r = a_1\epsilon^{1/2}(t - t')^{3/2}/(1 + a_2(t - t')/T_L)$. Similarly, we compute the GLC C for the same release but for the meandering puffs with $\sigma_x = \sigma_y = 0.6w_*(t-t')/(1+0.5(t-t')/T_{Lx})^{1/2}$ and $T_{Lx} = 0.7h/w_*$. For an infinitely-long release, the C_c and C values should reduce to those for a continuous plume as shown below; thus the plume results serve as an upper bound to the concentration values for the short-duration release.

The mean concentration field relative to a plume centerline is given by

$$C = \frac{Q_r}{2\pi U\sigma_{ry}\sigma_{rz}} \exp\left(-\frac{y^2}{2\sigma_{ry}^2} - \frac{(z - h_e)^2}{2\sigma_{rz}^2}\right) . \tag{12}$$

Here, the plume rise is attributed to buoyancy and is given by $\Delta h = 1.6F_b^{1/3}x^{2/3}/U$ and its radius is $r = 0.4\Delta h$ (Ref. 17). Source momentum effects can be included in the future. As with the puff model, we will assume $\sigma_{ry} = \sigma_{rz} = \sigma_r$ and $\sigma_r^3 = \sigma_{rb}^3 + \sigma_{ra}^3$. The σ_{ra} is given by Eq. (11) and the plume $\sigma_{rb} = r/\sqrt{2} = 0.45F_b^{1/3}x^{2/3}/U$. The $C_c = Q_r/(2\pi U\sigma_r^2)$ from Eq. (12); these expressions are expanded to include reflection at $z = 0, h$.

Example Results

Results are presented for the dimensionless concentration C_cUh^2/Q_r for the plume and integrated-puff models, with reflection at $z = 0, h$ included in both. The buoyancy of the continuous source is characterized by the dimensionless buoyancy flux (Ref. 10):

$$F_* = \frac{F_b}{Uw_*^2h} , \tag{13}$$

where F_b is the source buoyancy flux which is proportional to the source heat flux.

Figure 3 shows the C_cUh^2/Q_r as a function of X for the plume model with F_* in the range $0.001 \le F_* \le 0.3$. The large variation in the dimensionless C_c at short range ($X < 1$) is due to the buoyancy-induced dispersion σ_{rb}. As can be seen, C_cUh^2/Q_r decreases systematically and significantly with an increase in F_* due to the increase in σ_{rb} with F_*. For $X > 1$. the curves converge to the same limit because at long times the σ_r is dominated by σ_{ra}, which is independent of F_*.

Figure 4 presents the C_cUh^2/Q_r for both the plume and integrated-puff models for $F_* = 0.01$ and various values of $t_{r*} = t_rw_*/h$. the dimensionless release duration. The time

scale $h/w_* = 500$ s for the w_* (= 2 m/s) and h (= 1000 m) used here, so that t_r ranges from 50 s to 500 s or about 1 to 8 min. As can be seen, the plume result (solid curve) is an upper bound to the integrated-puff model results. The X value corresponding to the departure of the integrated-puff solution from the plume solution increases as t_{r*} does. For $X \geq 5$, the integrated-puff concentrations can be significantly less than the plume concentrations; this is due to the finite duration of the source.

Figure 5 shows the dimensionless mean GLC, CUh^2/Q_r, for the meandering plume and for a sequence of meandering puffs (finite-duration release). The trends with X and t_{r*} are similar to those in Fig. 4, but the near-source variation of CUh^2/Q_r with X differs from that for C_c due to the different dispersion rates in relative (Fig. 4) and absolute dispersion (Fig. 5). Note that at $X = 0.1$, the GLC value is about an order of magnitude smaller than the C_c (Fig. 4) because the ground is significantly removed from the elevated plume centroid. However, at $X = 10$, the concentration values are quite similar; this occurs because the concentration distribution becomes uniform in the vertical due to plume trapping and the horizontal spreads (relative and absolute) are about the same.

ACKNOWLEDGMENTS

This work has been supported by the DOD/DOE Strategic Environmental Research and Development Program. We are grateful to Seth White for producing the figures.

REFERENCES

1. Andrulis Research Corporation, *Development of methodology and technology for identifying and quantifying emission products from open burning and open detonation thermal treatment methods. Bangbox test series*, Vol. 1, Final Rpt., U.S. Army Armament, Munitions, and Chemical Command, Rock Island, IL, 1992.

2. W.B. Petersen, "A demonstration of INPUFF with the MATS data base," *Atmos. Environ.*, 20: 1341 (1986).

3. J.C. Weil, B. Templeman, R. Banta, and W. Mitchell, "Atmospheric dispersion model development for open burn/open detonation emissions," in ***Proceedings AWMA 88th Annual Meeting & Exhibition***, 95-MP22A.05, Air and Waste Management Association, Pittsburgh, PA, 1995.

4. G.A. Briggs, "Some recent analyses of plume rise observations," in *Proceedings of the Second International Clean Air Congress*, H.M. Englund and W.T. Beery, Eds., Academic Press, NY, 1971, pp 1029–1032.

5. J.C. Wyngaard, "Structure of the PBL," in *Lectures on Air Pollution Modeling*, A. Venkatram and J.C. Wyngaard, Eds., Amer. Meteor. Soc., Boston, 1988, pp 9–61.

6. A. Venkatram and J.C. Wyngaard. Eds.. *Lectures on Air Pollution Modeling*. Amer. Meteor. Soc., Boston, 1988.

7. S.G. Perry, A.J. Cimorelli, R.F. Lee, R.J. Paine, A. Venkatram, J.C. Weil, and R.B. Wilson, "AERMOD: A dispersion model for industrial source applications," in *Proceedings AWMA 87th Annual Meeting & Exhibition*, 94-TA23.04, Air and Waste Management Association, Pittsburgh, PA. 1994.

8. G.T. Csanady, *Turbulent Diffusion in the Environment*, Reidel, Dordrect, 1973.

9. J.C. Weil, R.I. Sykes, and A. Venkatram, "Evaluating air-quality models: review and outlook," *J. Appl. Meteor.*, 31: 1121 (1992).

10. J.C. Weil, "Dispersion in the convective boundary layer," in *Lectures on Air Pollution Modeling*, A. Venkatram and J.C. Wyngaard, Eds., Amer. Meteor. Soc., Boston, 1988, pp 167–227.

11. R.I. Sykes, "Concentration fluctuations in dispersing plumes," in *Lectures on Air Pollution Modeling*, A. Venkatram and J.C. Wyngaard, Eds., Amer. Meteor. Soc., Boston, 1988, pp 325–356.

12. F.A. Gifford, "Statistical properties of a fluctuating plume dispersion model," *Adv. Geophys.*, 6: 117 (1959).

13. R.S. Scorer, *Environmental Aerodynamics*, Halsted Press, NY, 1978, pp 276–303.

14. J.C. Weil, "Source buoyancy effects in boundary layer diffusion," in *Proceedings of the Workshop on the Parameterization of Mixed Layer Diffusion*, R.M. Cionco, Ed., Physical Science Laboratory, New Mexico State University, Las Cruces, NM, 1982, pp 235–246.

15. J.R. Richards, "Experiments on the penetration of an interface by buoyant thermals," *J. Fluid Mech.*, 11: 369 (1961).

16. D.J. Thomson, "A stochastic model for the motion of particle pairs in isotropic high-Reynolds-number turbulence, and its application to the problem of concentration variance," *J. Fluid Mech.*, 210:113 (1990).

17. G.A. Briggs, "Plume rise and buoyancy effects," in *Atmospheric Science and Power Production*, D. Randerson, Ed., U.S. Dept. of Energy DOE/TIC-27601, 1984, pp 327–366.

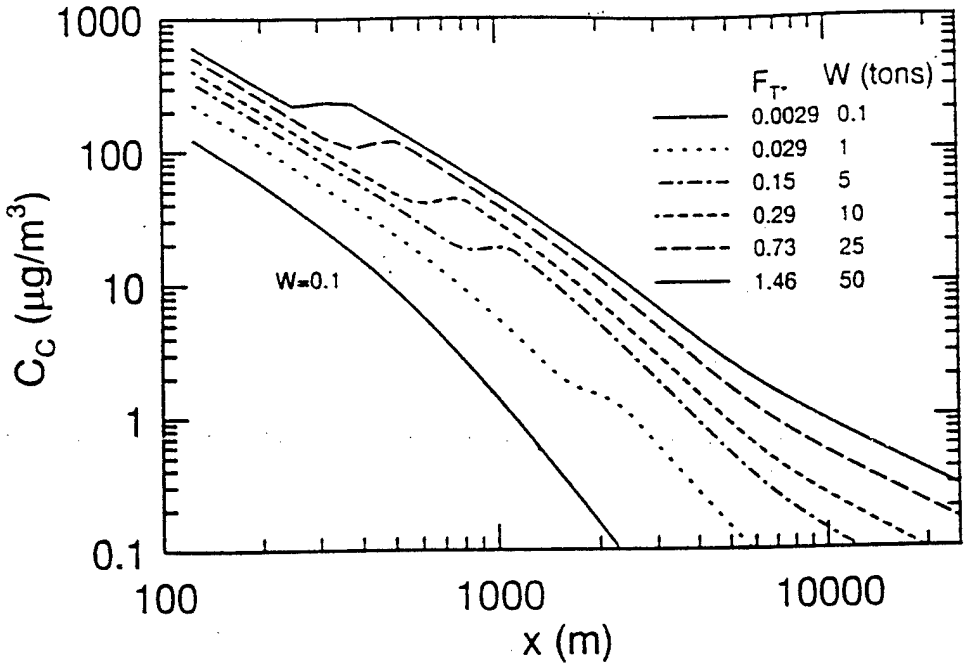

Figure 1. SO_2 concentration at detonation cloud centroid as a function of downwind distance and detonation mass W.

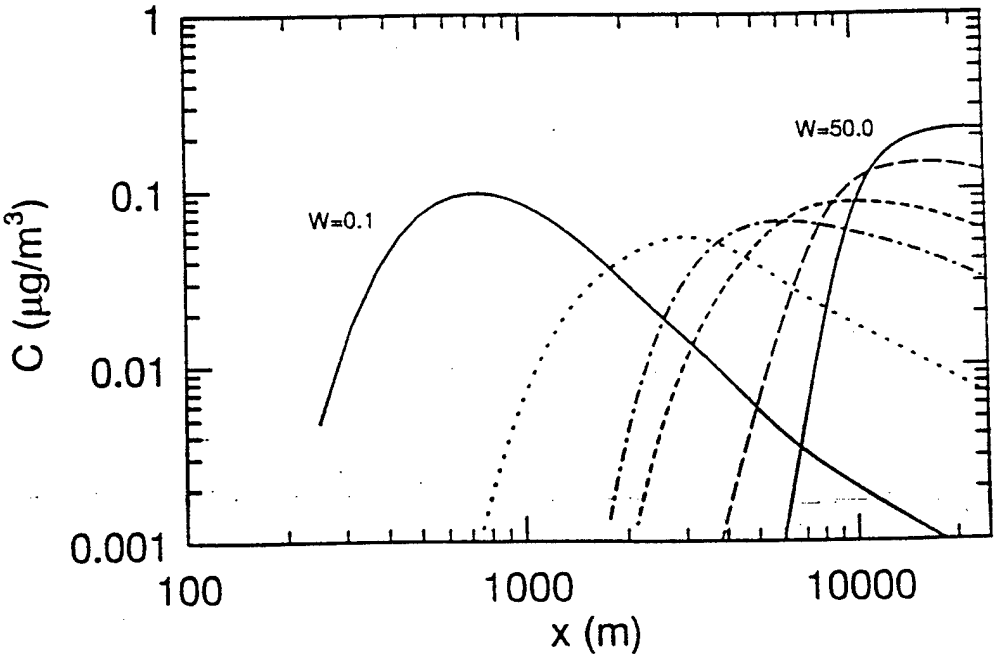

Figure 2. Mean ground-level SO_2 concentration along puff centerline as a function of downwind distance and detonation mass; see Fig. 1 for key to lines.

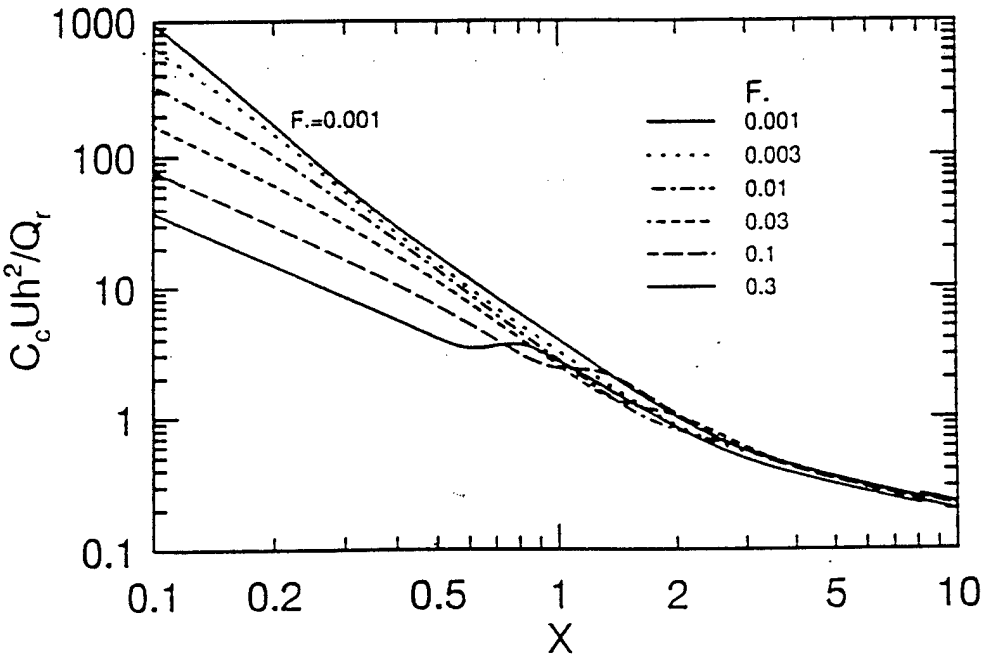

Figure 3. Dimensionless concentration at plume centroid as a function of dimensionless downwind distance and dimensionless buoyancy flux F_*.

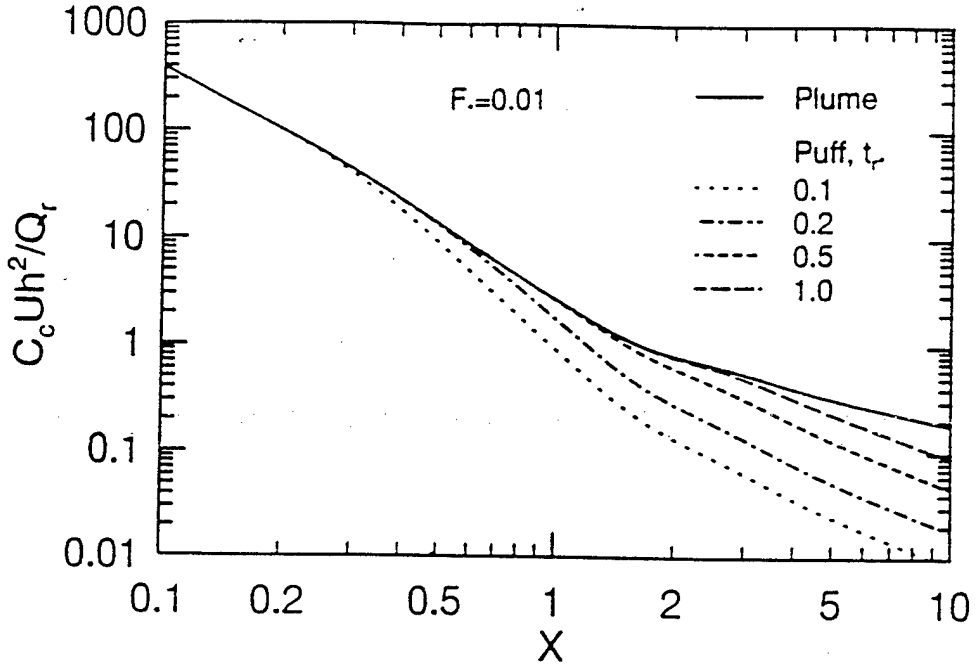

Figure 4. Dimensionless concentration at plume or puff centroid as a function of dimensionless downwind distance and dimensionless release duration t_{r*}.

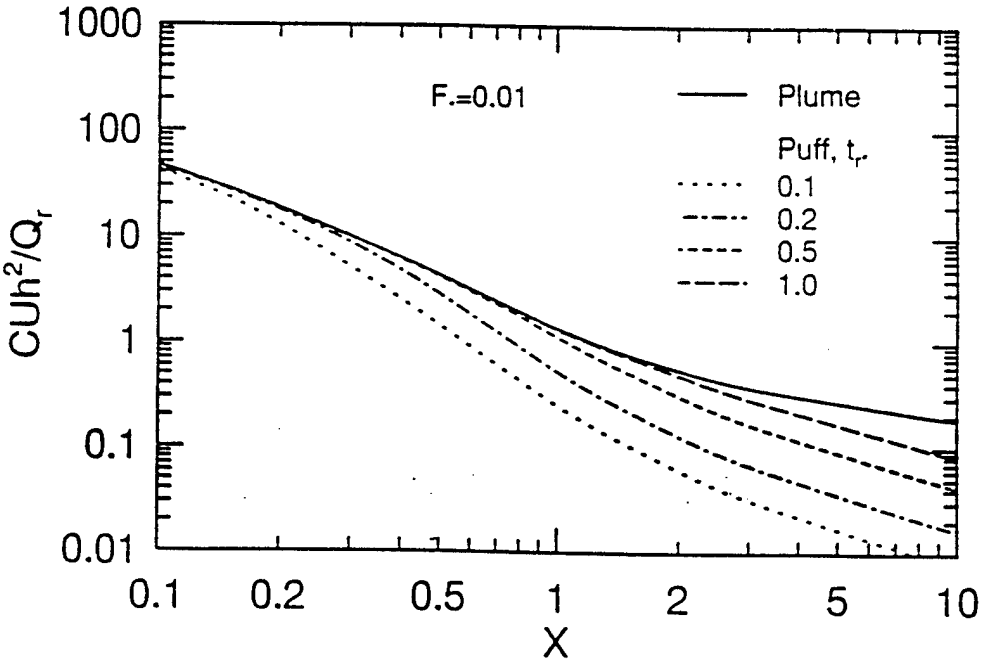

Figure 5. Dimensionless mean ground-level concentration along plume or puff centerline as a function of dimensionless downwind distance and dimensionless release duration t_{r*}.